Factors Affecting Frequency Content in preSDM Imaging

Ian F. Jones
&
Juergen K. Fruehn

'The Leading Edge'
v22, No.2, pp 128-134

GX Technology
Lawrence House
45 High Street, Egham
Surrey TW20 9DP
UK
Tel: +44 1784 497630
Email: ijones@gxt.com

Factors Affecting Frequency Content in preSDM Imaging

Ian F. Jones & Juergen K. Fruehn
GX Technology EAME, Lawrence House, 45 High Street , Egham, Surrey TW20 9DP, UK

Introduction

It is sometimes remarked that pre-stack Kirchhoff depth migrated images have a lower frequency content than their time-domain counterparts. Various factors that influence frequency content during migration are evaluated, with the object of assessing the reasons for potential loss of bandwidth in migrated data.

In the following examples, the nature and cause of these various factors that can impact the frequency content are summarized. The factors are examined to determine their effects on depth migration more than on time migration, or Kirchhoff migration more than wavefield extrapolation schemes.

We believe that there is no inherent reason for the bandwidth of Kirchhoff depth migrated data to be worse than other migrated data, by demonstrating and offering recommendations to ensure optimal frequency content in the processed output image.

The analysis covers the following topics:
- Spurious Differences
- Aliasing: Temporal & Spatial
- Wavelet Changes During Migration:
  Frequency, Velocity & Offset Dependent
- Kirchhoff Migration as a Stacking Process:
  Travel-Time Sampling Errors;
  Sensitivity to Velocity Error;
  Acquisition Footprints

Spurious Differences

It would be instructive to re-state some obvious aspects of this exercise. For example, a common element of confusion in time versus depth comparisons is the degree of post processing. A final time product (with its associated deconvolution and spectral balancing) will naturally look better in terms of signal content, than a raw time-converted preSDM result. Consequently, it is important to perform the appropriate post processing on output from the preSDM before drawing any conclusions. In the case of designing spectral balancing operators, we must ensure that the preSDM output spectrum extends well beyond the signal spectrum.

While a frequency-domain Finite Difference algorithm explicitly limits the frequency range (Fmin & Fmax parameters), a time-domain Kirchhoff approach does not inherently limit the frequency range. However, in preparation for anti-alias filtering or variable depth step, some Kirchhoff schemes may require band limiting the data. Thus, in comparative analysis, we must ensure that we are comparing data sets with the same frequency bandwidth.

Figure 1: In the raw preSDM output, the target horizon (faulted sandstones) lying beneath an unconformity appears to have a lower frequency bandwidth than the conventional preSTM result. However, applying similar wavelet processing to the preSDM produced a superior result. Depth results shown are converted to time.

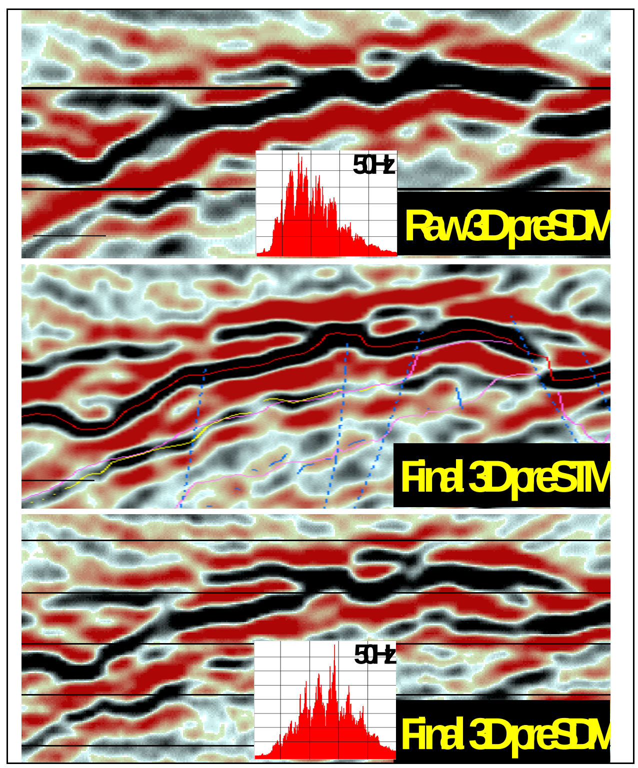

Temporal Aliasing

Re-sampling the time data from 2 ms to 4 ms for subsequent data processing is common practice. To avoid aliasing the signal with energy beyond the Nyquist frequency, the time data needs to be pre-filtered properly. Likewise, during depth migration, we must ensure that we don't alias the temporal frequencies that were not adequately sampled by the output depth step.

This is usually not a problem for Finite Difference depth migration, as we band-limit the data explicitly during migration. In contrast, Kirchhoff migration does not have an explicit time-frequency cut-off. We must therefore ensure that upon output, no aliased energy survives.

To accomplish this, we must pre-filter the input time data by calculating the frequencies permissible in the output depth data through the simple relationship between dz (output depth sample rate for migration) and Vi(t) (interval velocity function). The maximum temporal frequency that can be imaged for a given dz is:

$$F_{nyq} = Vi/(4*dz)$$

For example, the typical shallow marine data imaged with a 10-m depth step, would require the input data to be pre-filtered to about 35 Hz in the shallow section:

Two-way time (ms)	Vi (m/s)	F_{nyq} (Hz)
200	1600	40
1000	1800	45
2000	2000	50
3000	3000	75
4000	3600	90

This filtering is counter-intuitive, as we usually think of applying and keeping a higher frequency bandwidth in the shallow section.

The problem of not having pre-filtered the data to guard against temporal aliasing is only important when we image at a 10-m depth step (or greater) or in shallow marine environments with low velocities. At greater depths or employing a 5-m depth step, the problem is not as severe. For land data, the problem usually doesn't occur since the near-surface has much higher velocities. However, problems can be severe in shallow unconsolidated areas, such as sand dunes, where surface velocities are low.

In Figure 2, we see the effects of imaging at 10-m depth step without (2a) and with (2b) appropriate pre-filtering. Figure 2c shows the vertical wavenumber spectrum with and without aliasing.

Figure 2a

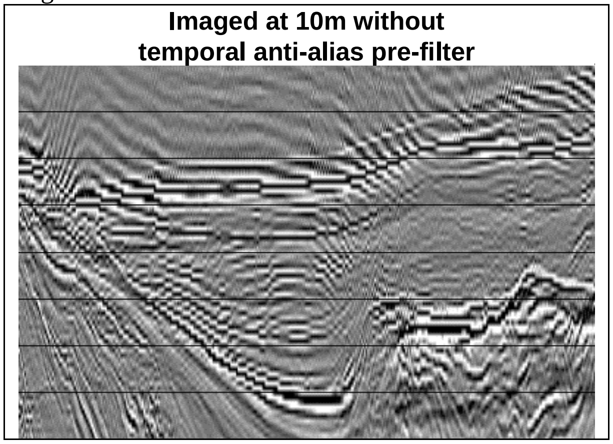

Figure 2b

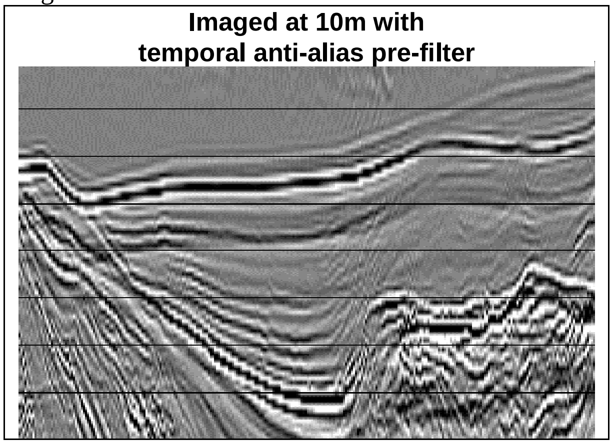

Figure 2c

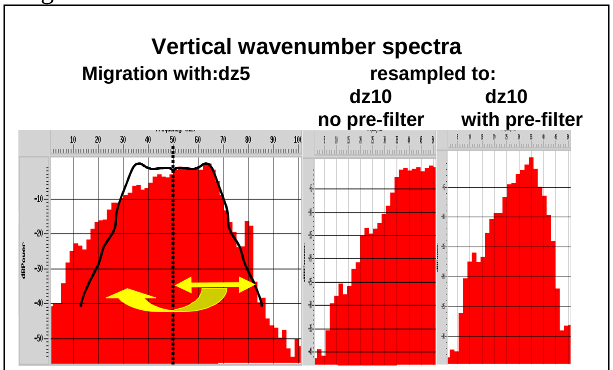

All energy above 50m^{-1} is aliased back onto the useful part of the spectrum if we fail to de-alias the data before re-sampling (or migration)

Recommendations
Estimate the global minimum 1D velocity function that is representative of the 3D velocity field. Compute the corresponding Fmax for the depth step to be used in the migration. Pre-filter the data with the appropriate low-pass filter.

Parameter testing (design of aperture, spatial anti-alias filter, etc) must be performed only on data that have been appropriately pre-filtered.

Spatial Aliasing
During migration, data is moved out along the impulse response to increasingly higher dips, prior to summation to form the output image. For a given inter-trace distance, a given frequency will become aliased for a given dip. In order to prevent the aliased frequencies from being summed into the output image, we apply an anti-alias filter during migration.

This will limit the frequency content of dipping reflectors. This observation is true for all migrations, but is more pronounced in Kirchhoff migration, where we explicitly apply an anti-alias filter.

For Finite Difference migration schemes in time, we do not usually have explicit control of the operator, but aliased frequencies will be rejected as evanescent energy.

For a time domain signal, the aliasing threshold is given by (Yilmaz, 1987)

$$F_{max} = V/(4.\Delta x.\mathrm{Sin}(\vartheta))$$

where ϑ is the structural dip, Δx is the output intertrace, V is the velocity, and Fmax is the maximum non-aliased frequency.

The alias condition is more complicated in the depth domain due to the depth (velocity) dependent nature of the frequency.

Sometimes the design of the anti-alias operator is sub-optimal, as the effect of tapers is not properly taken into account, and the filter kills too much high frequency energy. Thus, omitting the anti-alias filter can sometimes give a better result, especially at greater depths where high-frequency aliased energy is less of a problem.

In Figures 3a and 3b, a salt diapir is presented where anti-aliasing improves the shallow section but degrades the deeper parts of the image, after migration using parameters selected to best image the shallow section.

Recommendations
Produce a test line with the anti-aliasing turned-off, so as to be able to assess any potential damage done to steep dips by the choice of anti-alias parameters. Adjust the anti-alias parameters accordingly.

Figure 3a: Image quality is improved in the near surface of this salt diapir by application of spatial anti-aliasing. However, using ‘default’ parameters, deeper events are degraded.

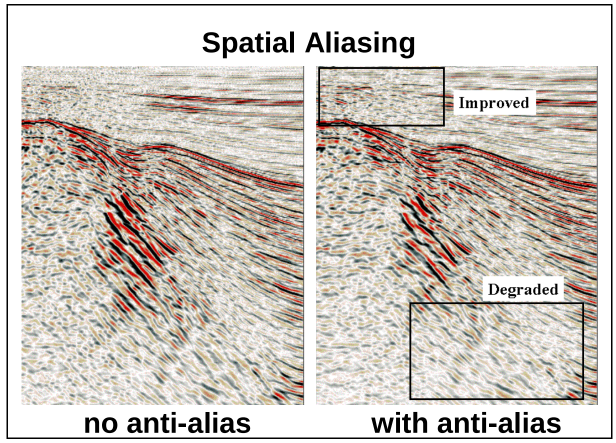

Figure 3b: enlargement of deep events

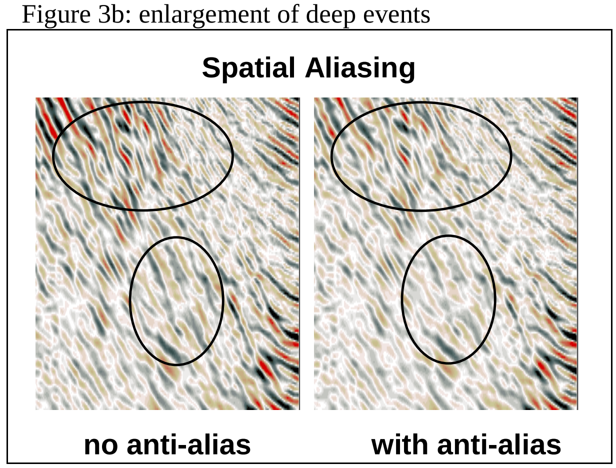

Wavelet changes during migration:

We have various ‘legitimate’ changes to the character of the seismic wavelet during migration, in proportion to dip, velocity contrast, and offset. However, as seen in Figure 4, where we compare a small segment of flat data after various processing steps, we note that nothing unusual happens to the wavelets. In other words, for these synthetic data with a known model, time and depth imaging give comparable results in terms of frequency content.

Frequency Dependent Changes

In general, migrating a dipping structure will lower the frequency content of that event. This outcome is common in both time and depth migrations, but care must be taken to properly choose the low-cut filter displays so as to preserve the post-migration frequency content of the data.

Figure 4: The spectrum of each processed data example is shown in red. The black spectral envelope is the spectrum of the input wavelet. Other than a slight downshifting in the bandwidth due to stacking effects, the time and depth migrations give comparable results in terms of frequency content.

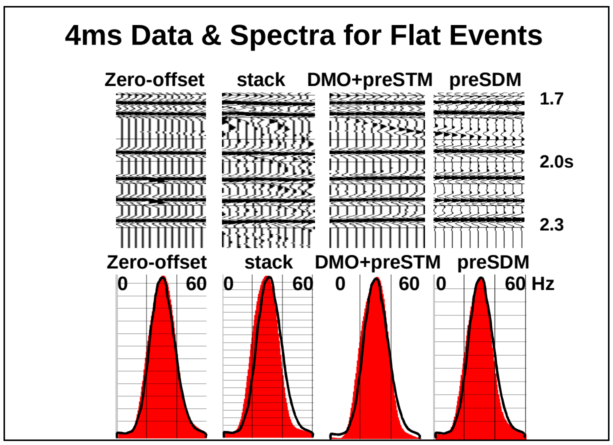

Figure 5 shows the effect for a simple dipping event: the wavelet is stretched during time migration, and a corresponding stretch occurs in depth migration. The lowering of frequency is proportional to the dip.

This also has a corresponding effect on the design of deconvolution operators. It can be observed that using a deconvolution whose parameters have been chosen by testing on a time migrated image, will give a sub-optimal result when used on a depth migrated image (converted to time).

Recommendations

Deconvolution tests and parameter selection should preferably be done on the depth migrated data (converted back to time) rather than applying deconvolution operators with parameters selected from previously existing time migrated data.

Velocity Dependent Changes

On a time migrated section, the wavelet is seen in its domain of measurement. Ignoring the effects of dispersion and attenuation, the wavelet will appear stationary down the trace with its phase and frequency content remaining the same.

Figure 5: The frequency content of a dipping reflector is downshifted in proportion to Cosine(dip) during migration.

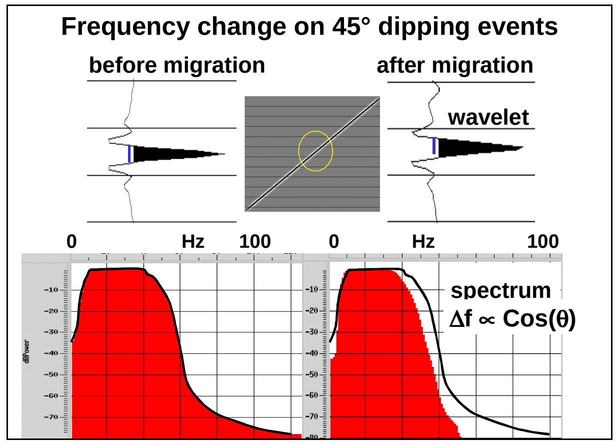

On a depth migrated image however, the wavelet is seen in depth, and its wavelength changes in accordance with the velocity contrasts it sees. The wavelet is stretched as it passes through an interface with a high velocity contrast.

Consequently, the wavelets appear to be of lower frequency in the deeper parts of the section in the depth image. This stretch effect can be removed by a vertical stretch back to time, and if we do this, the frequency content of the wavelet should be similar to that of a time image.

Although, we have stated that converting back to time will 'back out' the vertical wavelet stretch, on real data, life is not so simple. Due to the persistence of RMO, the depth domain wavelets are not perfectly aligned in the CRP gathers. Thus upon stacking, we degrade the wavelet character. This distorted wavelet is then converted back to time with a model whose velocity interface sits 'somewhere' within the distorted wavelet. Thus, a residual low-frequency element remains in the wavelet after conversion back to time. If the input data are minimum phase, then this effect can be lessened somewhat, as the energy of the wavelet is front-loaded. There is also the interplay with where the horizon boundary sits within the wavelet.

Recommendations
Strive towards a good wavelet compression sequence prior to migration.

Offset Dependent Changes
A more problematic, and fundamental problem related to depth imaging, is the offset dependent stretch of the wavelet in depth (Tygel, et al, 1994, 1995). This is analogous to the NMO stretch in time processing (Barnes, 1995).

In the depth domain, the severity of the stretch is proportional to the incidence angle, reflector dip, and to the velocity (Figure 6). Hence the effect is very noticeable for the farther offsets (figure 7). In addition, the effect stands out at high velocity contrast layers, especially after a velocity inversion, as in this case, the downgoing rays refract back to the vertical, thus reducing the angle of incidence of subsequent reflections. Consequently, the stretch at the base of the high-velocity layer appears more pronounced in comparison to deeper events. Hence the effect is most noticeable at unconformities, carbonate, and salt interfaces (Figures 8a and 8b).

Because the stretch can both increase and decrease with depth, such events are difficult to mute out with a standard processing mute, as the mute functions often must be monotonic. To deal with depth stretched wavelets, we need to design an automatic stretch dependent mute.

With respect to the zero-offset trace, the stretch factor is given by:

$$Mo = 2Cos(\vartheta)Cos(\beta)/V,$$

where V is the upper medium velocity, ϑ is the incident angle for this offset, and β is the reflector dip

For increasing depth, the dominant factor is the velocity.

Recommendations
Stacking mutes should be selected after preSDM. Consequently, the pre-migration mute should be left quite wide. Ideally, an automatic stretch mute, with a parameter to select the stretch threshold could be implemented.

This recommendation is only valid for offset domain Kirchhoff migration. In a wavefield extrapolation, shot migration scheme energy is mixed between offsets during the migration. Thus, the mutes must be selected and applied prior to migration.

Figure 6

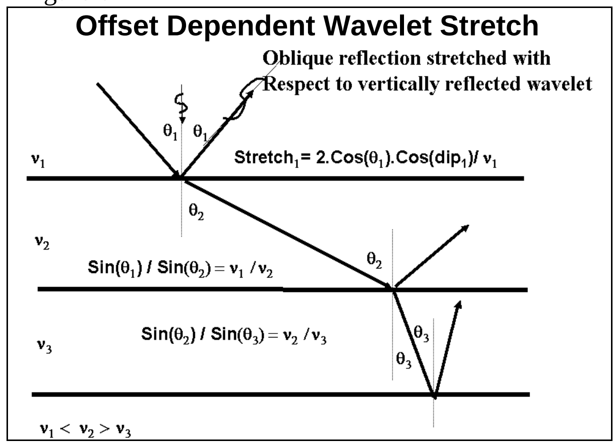

Figure 7: An offset dependent wavelet stretch on the depth migrated traces where noticeable changes occur on shallow events or at large velocity contrasts

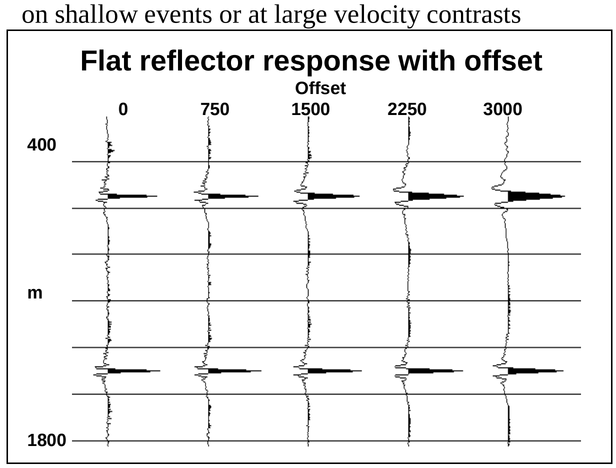

Figure 8a: The far offset wavelength is ~ twice the near offset wavelength.

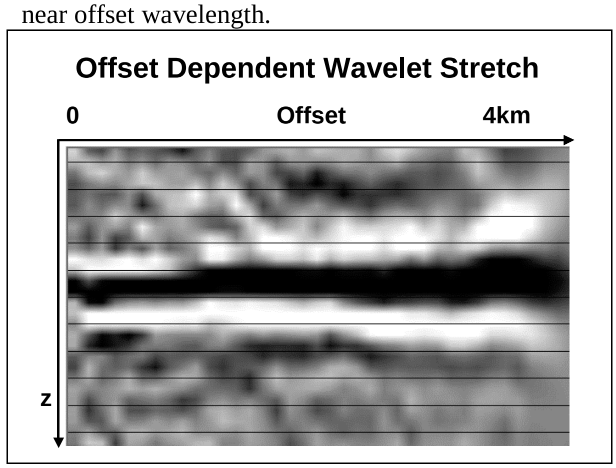

Figure 8b: Depth dependent (non-monotonic muting of the gathers can improve the character of the depth image.

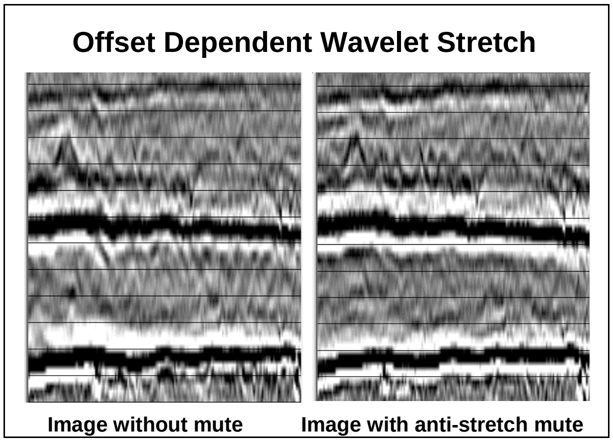

Kirchhoff Migration as a Stacking Process.
If we think of the migration as a sum over hyperbolic trajectories (in time migration) or over more complex asymmetric trajectories (in depth migration), then we can see that summing over an incorrect trajectory will lead to mis-stacking, which leads to a degradation of frequency content and amplitude.

Assuming we have the correct model, there will be 3 main influencing factors on image quality:

- Adequate sampling of the velocity field (i.e. travel times)
- Adequate sampling of the input data on the acquisition surface
- Adequate sampling within the Fresnel zone at the image point

Travel-Time Sampling Errors
There are various theoretical approximations made in ray-tracing or other travel time computation schemes, such as treating the curvature of a ray in a velocity gradient. However, a more mundane and damaging effect relates to how we sub-sample the travel times for storage.

In practice, the travel time calculation is performed by considering a five-dimensional problem:

- The 2D surface acquisition sampled at 125m x 125m grid, representing both the source and receiver positions, and
- The 3D subsurface volume sampled at 75m x 75m x 50m.

For each surface location on the 2D grid, we compute the one-way travel time to each of the nodes in the 3D subsurface volume (Figure 9). In general, the cost of computation increases as the cube of the depth (solving to a depth of 2km costs 8 times more than solving for a depth of 1km). Given that an input trace will not generally lie on the surface nodes used for calculation, we must therefore read the travel time tables associated with the four nearest neighbors and then interpolate. Also, given that the desired output points will not lie on the 3D volume nodes, we must also interpolate those values between nearest neighbors.

These interpolations introduce some errors. To avoid them, we should compute travel times for the true surface locations of all shots and receivers, and do so for all desired output depth samples (i.e. at the seismic sampling, typically 25m x 25m x 5m). However, the volume of space required to store all travel times is very large (i.e. a 10km x 10km x 10km volume = ~ 400 terabytes).

In the near surface, the travel time isochrons tend to have greater curvature, as the wavefield hasn't spread-out too much. If we sample the travel times on a surface grid of say 100m x 100m, and then interpolate these values down to 25m x 25m during the migration, we will have some interpolation error. If we use a simple linear interpolator to resample the travel times to the migration output grid spacing, then we will usually see a grid pattern artifact in depth slices through the resulting images in the shallow data (Figure 10).

Recommendations
QC the degree of artifact by inspecting 3D depth slices through the final image. The artifact is usually strongest at shallower depths, and can be mistaken for an acquisition 'imprint'. If necessary, use a non-linear interpolation and/or use the smallest 'affordable' grid;

Sensitivity to Velocity Error
As we have noted, an error in the travel times, due to whatever cause, results in mis-stacking in the Kirchhoff summation. This not only leads to a loss of stack power (Jones, et al, 1998), but also to a loss of frequency content. Both time migration and depth migration will suffer from loss of amplitude and frequency due to this mis-stacking.

However, depth migration is more sensitive to lateral velocity change (in fact, time migration ignores it to the extent that time migration operators are symmetric). Due to this greater sensitivity to velocity, a depth migration will suffer more than a time migration for a given velocity error.

Figure 9: Travel times are sampled on a 2D surface grid and ray traced to the nodes of the 3D subsurface image volume.

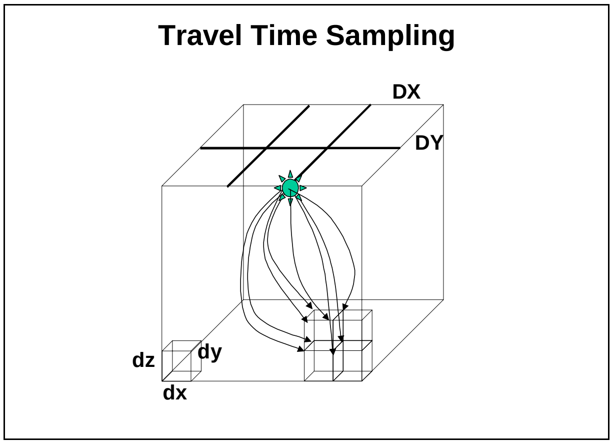

Figure 10: A grid pattern artifact is sometimes seen on shallow data due to travel time interpolation. This can be mistaken for an acquisition 'imprint'.

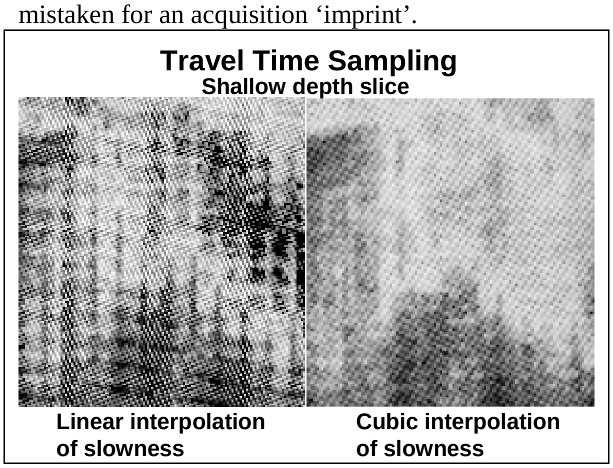

In Figure 11, synthetic data with small-scale length velocity anomalies are migrated first with the exact model, then with a smoothed model using both preSTM and preSDM algorithms. The preSTM result is similar with both models. PreSDM is worse with the smoothed model. The preSDM looses more frequency content that preSTM for small velocity errors.

Recommendations

Output all CRP gathers from the 3D preSDM final run. Then obtain a dense RMO velocity correction field – e.g. use an automatic velocity analysis tool to continuously analyze velocity along lines spaced at 100m: gathers can be converted back to time for this. Velocities can be output continuously along the lines, or subsampled to yield a 100m x 100m RMO correction grid, after appropriate editing and smoothing.

Figure 11: Velocity errors are more damaging for preSDM than preSTM.

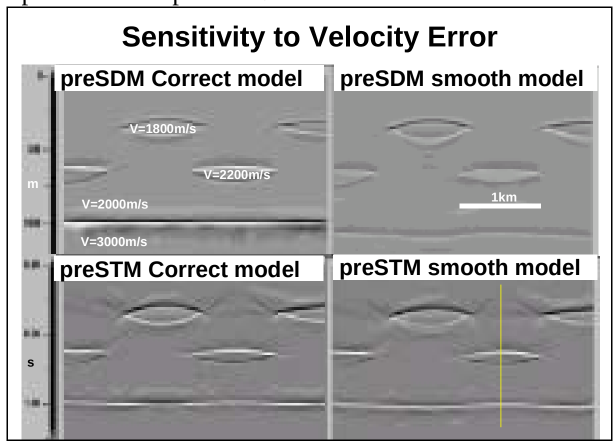

In order to quantify the extent of these effects, we consider a simple residual moveout problem, and assess the effects on the frequency content of the stacking of both the wavelet stretch and the RMO error.

After moveout correction, an event at 1s with RMS velocity 2km/s exhibits 80% wavelet stretch at 3km offset. The spectrum of such a wavelet is compared to that of the zero-offset trace in Figure 12. Stacking a correctly NMO'd gather gives the spectrum in Figure 13.

Figure 12: Spectra of near- and far-offset traces for a CMP after NMO of event at 1s two-way time with velocity 2km/s. Downshifting of spectra content during NMO is proportional to the far offset moveout, Δt_{NMO}

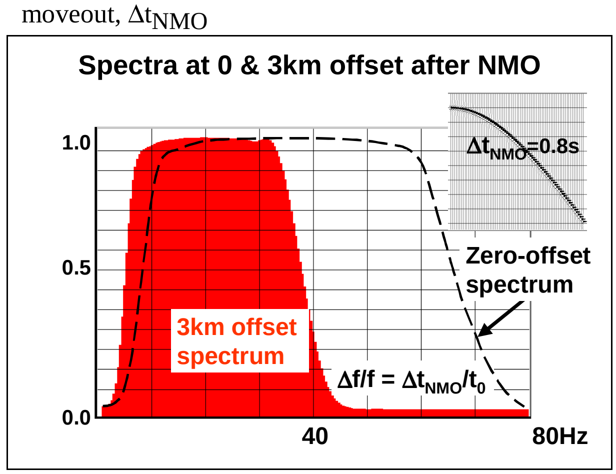

Figure 13

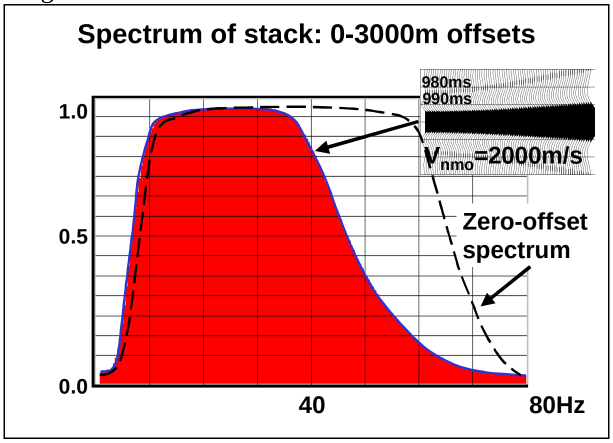

Figure 14: Both frequency content and amplitude are lost due to mis-stacking.

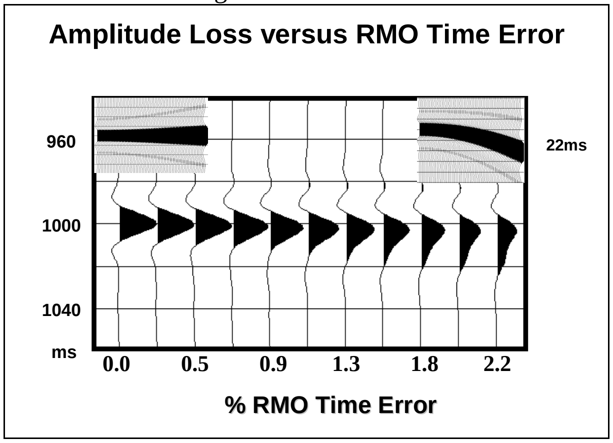

Figure 15: Spectra after stacking with progressively incorrect velocities.

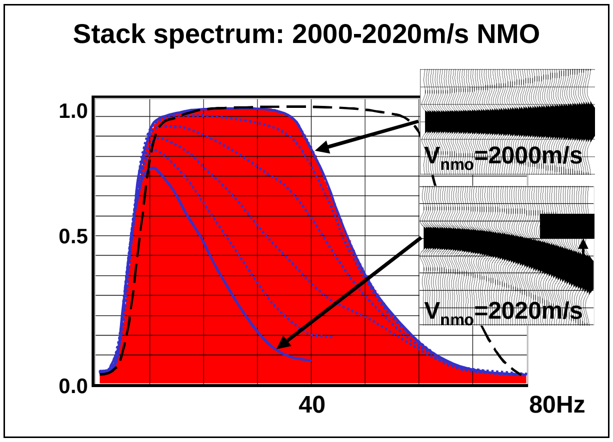

As we introduce moveout errors, the stack is degraded (see Figure 14) giving rise to a progressive loss in frequency content, as shown in Figure 15. This can be characterized by the stacking response curve in Figure 16.

Analogous processes happen during depth migration, where errors due to the travel time sampling of the velocity model, and to errors in the velocity model itself translate into travel time errors during Kirchhoff summation.

Figure 16: Loss of high frequencies as a function of % RMO time and % NMO velocity

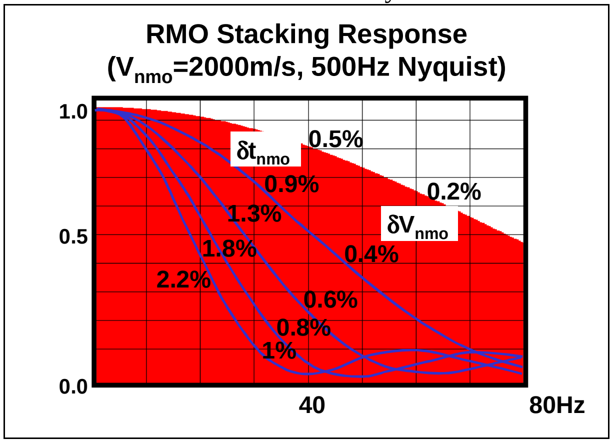

Acquisition Footprints

The theory of Kirchhoff migration assumes that the input data are regularly sampled in x, y, and offset, so that the resulting wavefield can be adequately reconstructed during imaging. If we have a gap in the input, there will be an amplitude anomaly in the output, as the corresponding Huygen's 'secondary wavelets' will not sum appropriately.

However, in practice we make use of the discreet nature of the integral implementation of a Kirchhoff scheme to migrate irregularly sampled data. This is one of the main attractions of Kirchhoff migration.

In the case of acquisition footprints, time processing is helped by bin-centered DMO and subsequent interpolation prior to migration. Finite Difference preSDM requires regular bin-centered input, so we avoid the problem as with time imaging.

Figure 17: Irregular input sampling gives non uniform amplitude behavior in the resultant image.

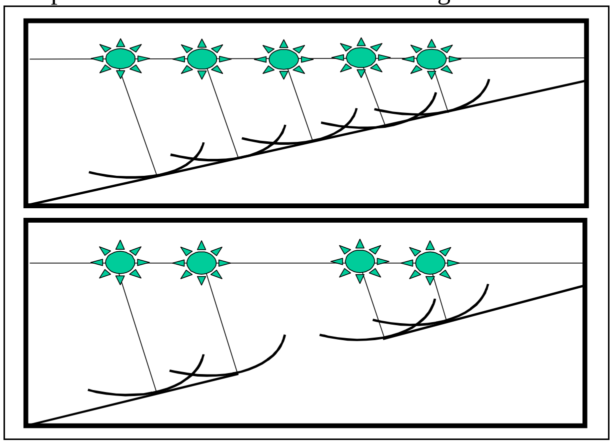

If the surface distribution is too irregular, and we do not want to accept the expense of pre-stack regularization, then a simple fold compensation-weighting scheme can be applied. This simply scales the input traces in proportion to their distance from their neighbours. This will fail if the gaps are too big, but can yield some improvements. Figure 18 shows the image of an unconformity at target level beneath a production platform, resulting in some coverage gaps, especially for short offsets. Fold compensation can reduce impulse response noise 'generated' by the holes.

Recommendations
Perform regularization/interpolation prior to Kirchhoff preSDM, or fold compensation.

Figure 18: Impulse response noise for data not pre-conditioned to compensate for surface sampling irregularity. The spectrum of the compensated data is broader in this case (but not always).

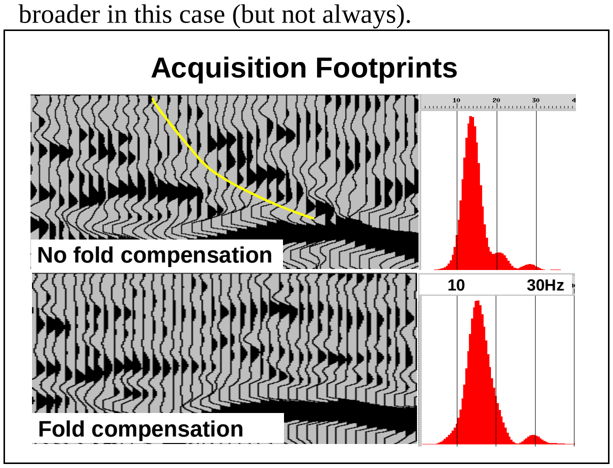

Conclusions
3D preSDM is still considered an expensive process; consequently, there is pressure to always find ways to "save money". However, if the savings result from compromises through improperly outputting and processing the full bandwidth gathers, then more money will be lost by having to work with sub-optimal images.

All gathers should be outputted from preSDM and the gathers should be subjected to the full conventional processing expected for any high-fidelity time-processing sequence (e.g. careful mute selection, wavelet deconvolution, signal spectral balancing, residual anti-multiple, etc).

A series of recommendations have been given in the body of the text. Following the majority of these recommendations, it should provide some guidance and safeguard against most of the factors that act to degrade depth image quality.

Acknowledgements
Thanks to TFE & bp, for kind permission to use their data, and to Mick Sugrue, Mike Bridson, Mike Goodwin, Nick Bernitsas, and Lawrence M. Gochioco of GXT for discussion, suggestions and some of the data examples. My thanks also to various colleagues at CGG for discussions related to this work, especially Antonio Pica, Keith Ibbotson, François Audebert & Pierre Plasterie.

References
Barnes, A. E., 1995, Discussion on 'Pulse distortion in depth migration', by M. Tygel, J. Schleicher, and P. Hubral (GEO-59-10-1561-1569): Geophysics, 60, no. 06, 1942-1947.

Jones, I.F., Ibbotson, K., Henry, B., Strachan, A., Baud, H., 1998, Enhancements to 3D preSDM salt-flank imaging, Journal of Seismic Exploration, v7, No.3/4, pp329-346..

Tygel, M., Schleicher, J., Hubral, P., 1994, Pulse distortion in depth migration: 64th Ann, Internat. Mtg. Soc. Expl. Geophys., Expanded Abstracts, 1359-1362.

Tygel, M., Schleicher, J. and Hubral, P., 1994, Pulse distortion in depth migration : Geophysics, 59, no. 10, 1561-1569. (* Discussion in GEO-60-6-1942-1949)

Yilmaz, O, 1987, Seismic Data Processing, SEG, Tulsa